Published by
NIGERIAN SOCIETY OF PHYSICAL SCIENCES
Available online @ https://asr.nsps.org.ng/index.php/asr

African Scientific Reports 4 (2025) 280

African Scientific Reports

Investigation of the spatial distribution of deterministic chaos in some meteorological variables across Nigeria

I. M. Echi, E. V. Tikyaa*, E. J. Eweh, A. A. Tyovenda, T. Igbawua

Department of Physics, Joseph Sarwuan Tarka University, Makurdi, Nigeria

Abstract

This study analyzes the spatial variation of the dynamical complexities in daily mean values of some meteorological variables over Nigeria using tools of nonlinear analysis such as correlation dimension, Lyapunov exponents and approximate entropy. Results obtained indicate low-dimensional deterministic chaos with Lyapunov exponent values ranging from 0.00181–0.0591 for precipitation, 0.00696–0.277 for wind speed, 0.00369–0.26 for temperature and 0.00109–0.00698 for all-sky radiation with locations in the north exhibiting higher degree of chaos in precipitation and air temperature as the Lyapunov exponents increased latitudinally while those in the south exhibit higher degree of chaos wind speed and all-sky radiation due to coastal effects. sCorrelation dimension values for precipitation showed insignificant spatial trends with values ranging from 0.106–2.34, wind speed (3.81–4.26), air temperature (3.55–4.25) and all-sky radiation (3.59–4.25) across the country. Furthermore, precipitation exhibited steadier repetitive pattern in the north with entropy values ranging from 0.359–0.837 while wind speed, air temperature and all-sky radiation showed less repetitive patterns along the border locations in the far north and coastal cities with entropy values ranging from 0.703–0.932, 0.724–0.892 and 0.718–0.877 respectively. The irregular trends are attributed to human anthropogenic activities, topography of these locations and variations in the Inter-Tropical Discontinuity.

DOI:10.46481/asr.2025.4.2.280

Keywords: Nonlinear dynamics, Chaos, Correlation dimension, Lyapunov exponents, Approximate entropy

Article History :
Received: 31 January 2025
Received in revised form: 07 June 2025
Accepted for publication: 04 July 2025
Published: 01 August 2025

1. Introduction

Chaos which is usually associated with the sensitivity of a deterministic system to minute perturbations in initial conditions. In 1961, Sir Edward Lorenz, a meteorologist accidentally discovered chaos in atmospheric systems with his crude model of atmospheric convection as it was heated from below by the ground. This hyper-sensitivity of some dynamical systems to initial conditions is sometimes called the 'butterfly effect.' The idea is that a butterfly flapping its wings in a South American rain-forest could, in principle, affect the weather in Texas. Lorenz realized that the chaotic nature of the atmosphere makes long-term weather prediction beyond just a few days difficult and "almost" impossible [1].

The light-weight and low viscosity of atmospheric air is responsible for the chaotic behavior of weather dynamics. It expands rapidly and randomly when in contact with hot surfaces and since air is a poor conductor of heat, the wind easily induces forced

*Corresponding author: Tel. No.: +234-703-209-6960.
Email address: evtikyaa@gmail.com (E. V. Tikyaa)

convections leaving the weather in an unstable equilibrium at all times [2]. Today, with the advancement and availability of sensors, computational weather forecasts rely on quantitative data about the current state of the atmosphere. Consequently, with scientific understanding of atmospheric processes, one can project how the atmosphere will evolve in future (*forecast*). Due to an incomplete understanding of the chaotic atmospheric processes, forecasts become less accurate as the range of forecast increases [3].

Plethora of literature are available on the mathematical concepts underlying the techniques for investigating chaotic phenomena and modeling of nonlinear dynamical systems. As such, several researchers have made efforts towards investigating the nature of the atmosphere by carrying out nonlinear dynamical analysis of weather observations at different locations. Joice and Thamilharazan [4] investigated the impact of the Tsunami on the atmospheric conditions related to the monsoon rainfall in Tamil Nadu, India. In their work, quantitative nonlinear analysis was carried out by calculating the Lyapunov exponents before and after the Tsunami. The Lyapunov exponent for the south-east monsoon rainfall in Tamil Nadu before and after the Tsunami was computed and found to be 0.285 and 0.799 respectively while that of the northeast monsoon rainfall was computed and found to be 0.5604 before Tsunami and 0.8606 after Tsunami. The increase in the values of the Lyapunov exponents suggest that the Tamil Nadu monsoon rainfall has certainly been disturbed by the Tsunami for the past few years.

Fathima and Jothiprakash [5] study the adaptability of the correlation dimension techniques for analyzing Indian rainfall data that is dominated by monsoon. The results obtained from the chaotic analysis revealed that correlation dimension method (CDM) is an efficient method for behavioral study of a time series. It also provides first-hand information on the number of dimensions to be considered for time series prediction modelling. The CDM applied to real life rainfall data brought out the nature of rainfall at Koyna station as chaotic. For the rainfall data, CDM resulted in a minimum correlation dimension of one and optimum dimension as five.

In Nigeria, Echi *et al.* [6] investigated the dynamics of rainfall and temperature in Makurdi from 1977 to 2010 using a variety of nonlinear techniques. Phase space reconstruction was done using optimal values of embedding dimension and time delay using the method of delays. Their results showed phase portraits with a distinct spongy-like structure geometry that indicates the presence of randomness and chaos in the meteorological time series. The correlation dimension values were estimated using the Grassberger-Procaccia algorithm and yielded 1.02 and 5.82 respectively for the rainfall and temperature. The Lyapunov exponents were calculated using Rosenstein's algorithm and the values were found to be 0.00832/day and 0.00574/day for daily mean rainfall and temperature respectively. The positive values of the largest Lyapunov exponents confirm the presence of chaotic dynamics in rainfall and temperature records over Makurdi and suggest predictability of within 112 days and 174 days for rainfall and temperature respectively. Fuwape *et al.* [7] investigated some nonlinear trends in rainfall and temperature data using quantifiers such as Lyapunov exponents, correlation dimension, and entropy for various locations across Nigeria and observed that for the locations in the south, positive Lyapunov exponents were obtained for the time series of mean daily rainfall for all locations implying deterministic chaos while in the north, negative Lyapunov exponents were obtained showing regular periodic behavior. The mean daily temperature data had positive Lyapunov exponent values ranging from 0.35–1.6 for all the locations sampled.

Similarly, in another work, Ogunjo *et al.* [8] investigated the nonlinear dynamics in global precipitation and temperature extremes using daily temperature range (DTR) and maximum 5-day precipitation (RX5) records. Their results were displayed as spatial maps constructed for the descriptive statistics of both DTR and RX5, and nonlinear parameters for Africa and South America. Their findings showed that the desert regions of Africa and South America exhibit lower complexity (determinism > 0.7) and higher persistence in RX5 values as compared with the other part of the continent. This was attributed to the dynamic atmospheric circulation patterns in the region. Other results showed the dynamics of equatorial West Africa and Congo River basin as less complex (determinism > 0.3) while the Brazilian highlands (determinism and laminarity > 0.5) were observed to be the highest in both DTR and RX5.

Adewole *et al.* [9] examined chaos in the trend of the meteorological parameters such as air temperature, relative humidity and wind speed in eight meteorological stations in Nigeria using nonlinear time series analysis techniques which include phase-space reconstruction, actual mutual information (AMI), false nearest neighbors (FNNs), and Lyapunov exponent. The delay time (τ) and embedded dimension (m) were determined using the methods of actual mutual information (AMI) and false nearest neighbors (FNNs) and found to be 10 and within the range of 5 and 9 respectively. With these, the optimum attractor reconstruction was obtained. Their results showed positive largest Lyapunov exponent across the eight stations which were found to be within the range 0.0034 - 0.1200 for all the parameters; indicating a strong presence of chaos. Ogunjo *et al.* [10] also investigated the dynamics of the River Niger discharge along two stations (Baro and Lokoja) located in Nigeria using the methods of phase space reconstruction, correlation dimension and Lyapunov exponent using the daily data for three periods spanning before and after the Kainji dam construction. The presence of deterministic chaos was confirmed with positive values of Lyapunov exponents in both locations, with the Lyapunov exponents at Baro in the range 0.0014–0.0150 while that of Lokoja ranged from 0.007–0.0145. Significant fractal values of correlation dimension values obtained at Baro (2.11–2.81) and Lokoja (2.28–4.51), a confirmation of low dimensional chaos with a forecast horizon for both locations in the range of 40–58 days into the future. This further buttressed the fact that chaos could be induced and its magnitude altered by human anthropogenic activities which directly affect the meteorological and hydrological system.

In this research, some quantitative tools of nonlinear dynamical analysis were deployed on daily mean values of experimental weather variables over Nigeria from 1982 to 2020 so as to characterize the dynamics of these meteorological variables and estimate the spatial distribution of deterministic chaos across the country in order to enhance more accurate longer-term prediction of the weather over Nigeria in the nearest future.

2. Theoretical framework

The quantitative tools of nonlinear analysis used to characterize the meteorological data in this paper include: Phase space reconstitution, correlation dimension, Lyapunov exponents and Kolmogorov-Sinai entropy.

2.1. Phase space reconstruction

Phase space reconstruction involves the drawing out of a multi-dimensional description of a system in an embedded space called state space from a univariate time series. Given a time series $\{y_1, y_2, ..., y_N\}$, its attractor (concentration of trajectories) can be reconstructed in an n-dimensional phase space of delay coordinates in form of the vectors [11, 12]:

$$Y_n = [y_n, y_{n+\tau}, y_{n+2\tau}, \ldots, y_{n+(m-1)\tau}], \tag{1}$$

where τ is the time delay, and m is the embedding dimension. The time delay τ is evaluated using the method of average mutual information (AMI) developed by Fraser and Swinney [13]. The AMI plot indicates the delay time of the time series as the value of the lag length at the first local minimum. Meanwhile the embedding dimension was computed using the method of false nearest neighbors (FNN) developed by Kennel *et al.* [14]. By computing and plotting the percentage of FNN against increasing embedding dimension, a monotonic decreasing curve is usually observed and the minimum embedding dimension can be evaluated from the point where the percentage of FNN drops to almost zero or a minimum value.

2.2. Correlation dimension (ν)

Correlation dimension is an evaluation of the degrees of freedom that describes the dynamics of the system [15]. It is also applied as a characteristic measure to distinguish between deterministic chaos and random noise [16]. The integer after the correlation dimension of a chaotic system is indicative of the minimum number of dependent variables required to model the dynamical system [17, 18]. In this study, the Grassberger-Procaccia algorithm is used to compute the correlation dimension. For any set of M points in an m-dimensional phase space, the correlation integral (spatial correlation of points) $C(r)$ is computed by the equation [19]:

$$C_m(r) = \lim_{N\to\infty} \frac{2}{N(N-1)} \sum_{i=1}^{M} \sum_{j=i+1}^{M} H\left(r - \left\|\overrightarrow{x_i} - \overrightarrow{x_j}\right\|\right), \tag{2}$$

where $H(x)$ is the Heaviside function, $\|\ldots\|$ is the Euclidean norm and r is the scaling parameter. For chaotic systems, the correlation integral power law for small values of r has the form [19]:

$$C(r) \sim r^{\nu}. \tag{3}$$

Thus by applying natural logarithm to both sides of (3), the correlation dimension ν is obtained as:

$$\nu = \lim_{r\to 0} \lim_{M\to\infty} \frac{\log C(r)}{\log r}. \tag{4}$$

Thus, constructing a log-log plot of the correlation integral versus a range of values of the neighborhood radius r, yields an estimate of the correlation dimension ν, which is evaluated by taking the slope of the linear regression line to the correlation dimension curve over a large range of r values [19].

In order to test the level of significance of correlation dimension values and distinguish between nonlinearity (deterministic chaos) and noise in the time series analyzed, a surrogate data technique was applied. The significance (S) of the difference is defined as [20, 21]:

$$S = \frac{\langle D_s \rangle - D_o}{\sigma_s}, \tag{5}$$

where D_o is the correlation dimension of the original data while $\langle D_s \rangle$ and σ_s are the mean value and standard deviation of the correlation dimension of the surrogate data sets which were generated using the Amplitude Adjusted Fourier Transform method in this research. It is expected that a positive value of S be returned since it is not likely that the randomized (surrogate) data are less random than the original data for nonlinearity to be confirmed [20]. In this work five surrogate data sets were simulated from the original time series for the surrogate test.

2.3. Lyapunov exponent (λ)

The Lyapunov exponent (λ) characterizes the rate of separation of infinitesimally close trajectories. It is mathematical expressed as [14]:

$$\lambda_1(i) = \frac{1}{i.\Delta t}.\frac{1}{M-i}.\sum_{j=1}^{M-i} \ln \frac{d_j(i)}{d_j(0)}, \tag{6}$$

where Δt is the sampling period of the time series, M is the number of reconstructed phase points and $d_j(i)$ is the distance between the j^{th} pair of nearest neighbors after i discrete-time steps.

A positive value of the Lyapunov exponent indicates chaotic behavior, a negative value indicates periodic behavior while a zero Lyapunov exponent indicates quasi-periodicity i.e. the system is in transition to chaos [21]. Rosenstein's algorithm was used in computing the largest Lyapunov exponent in this study [22]. Here, the Euclidean distance between i discrete time steps for each pair of neighbors is estimated using the expression:

$$d_j(i) = \left| Y_{j+1} - Y_{\widehat{j+1}} \right|, \text{ for } i = 1, 2, \ldots, \min(M-j, M-\widehat{j}). \tag{7}$$

The j^{th} pair of nearest neighbors diverges approximately at a rate equal by the largest Lyapunov exponent:

$$d_j(i) \approx C_j(i) e^{\lambda(idt)}, \tag{8}$$

where C_j is the initial separation of nearest neighbors (i.e. $d_j(0)$) and dt is the interval of sampling. Equation (8) could be expressed logarithmically as:

$$\ln d_j(i) \approx \ln C_j(i) + \lambda(idt). \tag{9}$$

Upon constructing a typical plot of the average log divergence ($\ln d_j(i)$) against the expansion step ($i.dt$), the slope of the linear fit to the long linear region prior to saturation gives an estimate of the largest Lyapunov exponent, λ [22].

2.4. Approximate entropy (ϕ)

The approximate entropy is a regularity statistic that quantifies the unpredictability of fluctuations and complexity within a nonlinear time series. It measures the degree of complexity and information loss in a system. Approximate entropy is computed by first generating a delayed reconstruction $Y_{1:N}$ for N data points with embedding dimension m, and time lag τ. Then the number of nearest neighbors within range at point i, are computed from the expression [23]:

$$N = \sum_{i=1,\ i\neq k}^{N} 1\left(\|Y_i - Y_k\|_\infty < R\right), \tag{10}$$

where 1 is the indicator function, and R is the radius of similarity.

The approximate entropy, ϕ is then calculated as:

$$\phi = \Phi_m - \Phi_{m+1}, \tag{11}$$

where

$$\Phi_m = (N-m+1)^{-1} \sum_{i=1}^{N-m+1} \log\left(N_i\right). \tag{12}$$

A relatively higher value of approximate entropy reflects the likelihood that similar patterns of observations are not followed by additional similar observations. Therefore, a signal containing highly repetitive patterns has a relatively smaller value of approximate entropy than a less predictable signal which has a relatively larger value of approximate entropy [24].

3. Study area and data source

3.1. The study area

Nigeria is located in West Africa and has coordinates $10°00'N$ (latitude) and $8°00'E$ (longitude). Nigeria is bordered by Benin Republic to the West, Cameroon and Chad to the East, Niger in the North and the Gulf of Guinea in the Atlantic Ocean to the South spanning a total land area of 923,768 km^2 and a population of about 188,660,253 [25]. It comprises of 36 states and the Federal Capital Territory, Abuja. There are three major ethnic groups in Nigeria: Hausa, Igbo and Yoruba with English as the lingua franca since Nigeria is a Commonwealth nation. However, Nigeria is a rich diverse ethnic entity encompassing 527 ethnic groups out of which 7 are extinct [26]. Nigeria comprises of five geo-climatic zones [27]. The zones are Sahel Savannah (Gusau, Sokoto, Maiduguri, Katsina and Damaturu), Sudan Savannah (Birnin-Kebbi, Dutse, Kano and Yola), Guinea Savannah (Abuja, Jalingo, Ilorin, Jos, Lafia, Lokoja, Makurdi, Minna, Kaduna, Bauchi, Gombe), Tropical Rainforest (Abeokuta, Ado-Ekiti, Akure, Ibadan, Oshogbo, Benin, Abakaliki, Asaba, Umuahia, Owerri, Awka and Enugu) and Coastal (Ikeja, Calabar, Port Harcourt, Uyo and Yenagoa). A map of Nigeria showing the six locations sampled is illustrated in Figure 1:

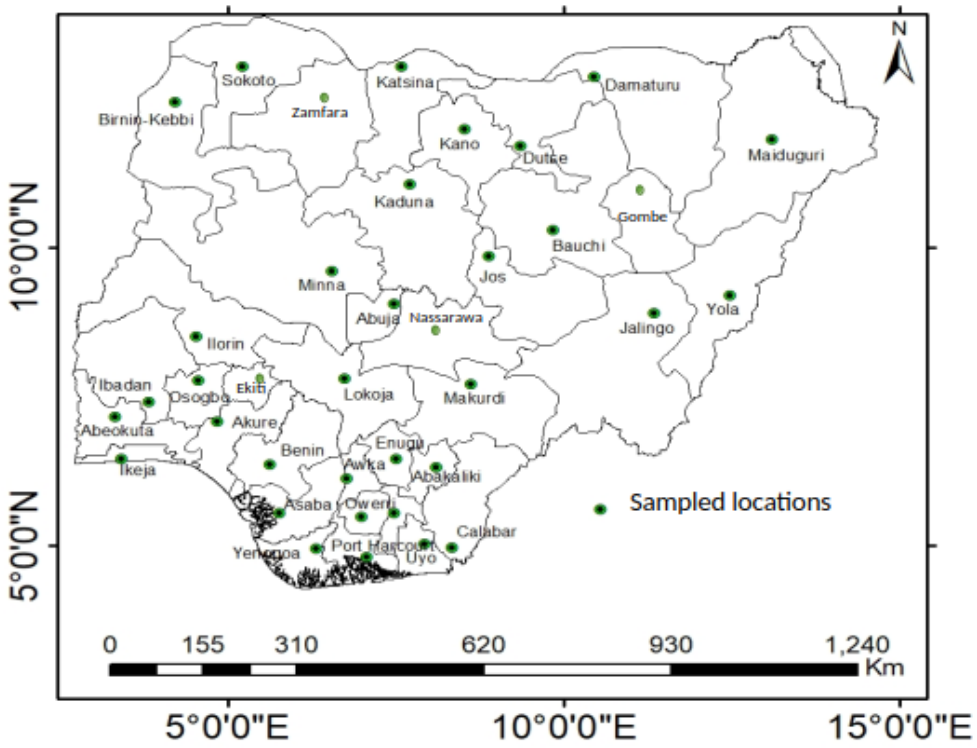

Figure 1: Map of Nigeria showing all the 37 locations sampled in this research [20].

3.2. The data source

The data used in this work was downloaded from satellite maps from the Modern Era Retrospective Reanalysis (MERRA-2) of the National Aeronautical and Space Administration (NASA) [28]. The meteorological data contains daily averages of precipitation (mm), wind speed (m/s), average temperature (°C) and all sky radiation (MJ/m^2/day) for the thirty-three locations across Nigeria from 1982 – 2020. Before the analysis was carried out, the trends and cyclic components in the data which are responsible for the seasonal variations, were removed by method of seasonal differencing. This renders the data stationary (zero mean, constant variance), thus revealing the deterministic components of the data which were then analyzed [16]. The seasonal and non-seasonal differencing equations used to remove trends and cyclic oscillations are given as [29]:

$$y_i = x_{i+1} - x_i, \tag{13}$$

$$Y_i = x_{i+m} - x_i, \tag{14}$$

$$DY_i = y_i \times Y_i, \tag{15}$$

where m is the seasonal lag which in this case is 365 days. DY_i is then applied to a filter operator (differencing polynomial) to get the stationary time series.

The nonlinear analysis was implemented using MATLAB (R2020a) while the mapping was carried out using the interpolation method was done in ArcGis 10.5 using the spatial Analyst tool box. The Inverse Difference Weighted (IDW) algorithm was adopted for this work. All the methods have their own skill and good at performing a certain kind of analysis. The IDW has an assumption that 2 points are related by the distance separation between them. It is given by [30]:

$$\widehat{z}(r_i) = \frac{\sum_{j=1}^{n} z(r_i)/d_{ij}^{p}}{1/\sum_{j=1}^{n} d_{ij}^{p}}, \tag{16}$$

where d_{ij} is the interval between the i^{th} and j^{th} points, $p = 2$ and its value can also be optimized by choosing the value which minimizes the absolute error [30].

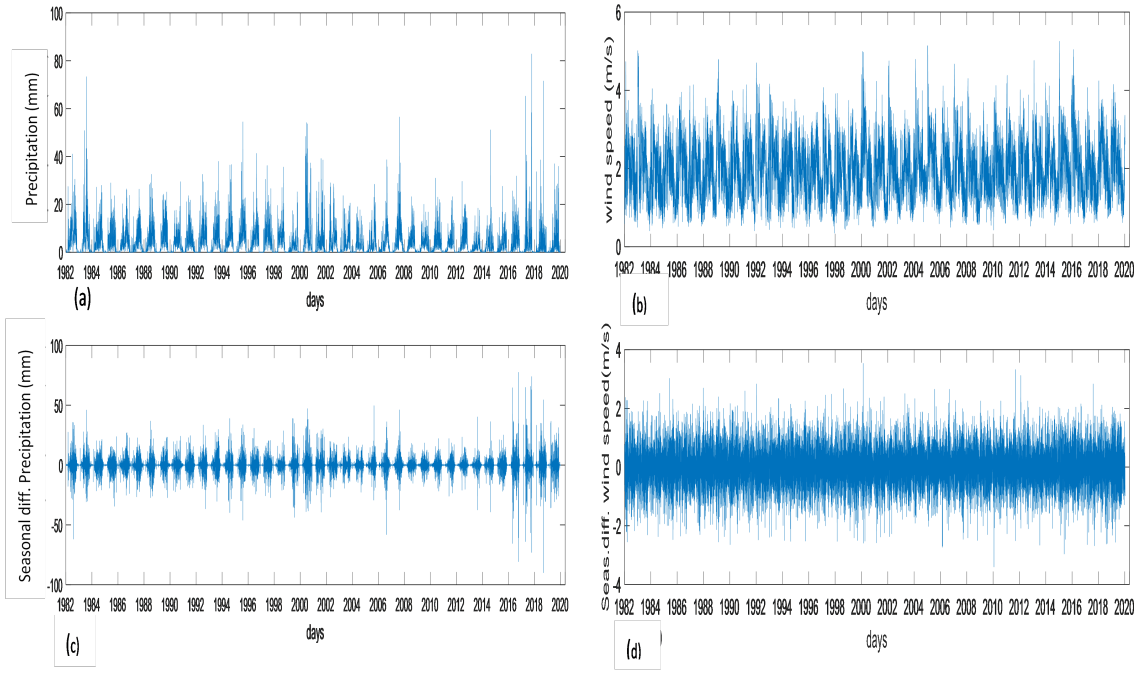

Figure 2: (a) Precipitation (mm) over Makurdi (b) Wind speed (m/s) over Makurdi from 1982-2020. (c) Seasonally differenced (stationary) precipitation over Makurdi (d) Seasonally differenced (stationary) wind speed over Makurdi from 1982-2020.

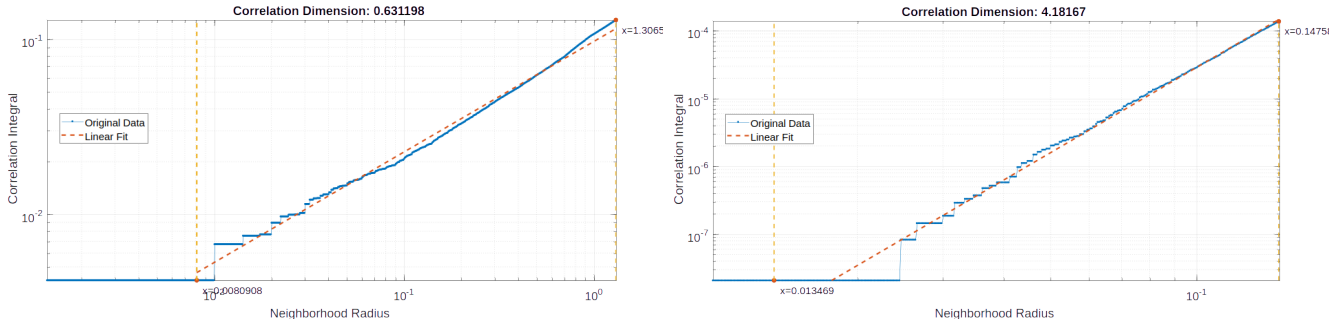

Figure 3: Estimation of correlation dimension using the Grassberger-Procaccia algorithm over Makurdi for: (a) Precipitation; $\nu = 0.631198$ by taking the linear fit in the neighborhood radius $0.0080908 \leq r \leq 1.3065$ (b) Wind speed; $\nu = 4.18167$ by taking the linear fit in the neighborhood radius $0.013459 \leq r \leq 0.14758$, from 1982-2020.

4. Results and discussion

4.1. Time series preprocessing and computational methods

A plot of the initial time series and the seasonally differenced time series plots for precipitation and wind speed over Makurdi from 1982 - 2020 are illustrated in Figure 2:

The procedure of estimating the correlation dimension using Grassberger-Procaccia algorithm is illustrated in Figure 3.

Lyapunov exponent computation via Rosenstein's method using MATLAB toolbox is shown in Figure 4.

4.2. Spatial distribution of mean values of the meteorological variables

The mean spatial distribution of precipitation, wind speed, temperature and all sky radiation is displayed in Figure 5. Their variation with latitude and longitude are also displayed in Figure 6. The coefficient of determination ($D = r^2$) was evaluated to check the significance of trends at 95% confidence interval with p values lower than 0.05. A near zero value of D indicates no relationship between the variables and thus an insignificant trend. The distribution of mean precipitation shows a significantly higher

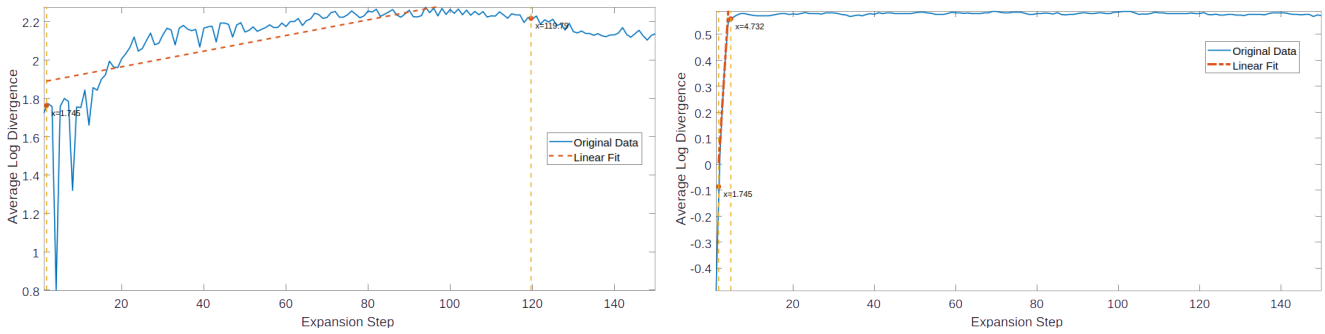

Figure 4: Estimation of the largest Lyapunov exponent using Rosenstein's Algorithm over Makurdi for: (a) Precipitation; $\lambda = 0.004033$ with linear fit expansion step $1 \leq r \leq 120$ (b) wind speed; $\lambda = 0.2606$ with linear fit expansion step $1 \leq r \leq 5$, from 1982-2020.

precipitation in the southern region and lower precipitation in the northern region of the country, with Calabar recording the highest mean precipitation of 7.972 mm, followed by wed by Yenagoa (7.498 mm) and then Port Harcourt (7.099 mm). The least mean precipitation was recorded in Damaturu (1.468 mm) followed by Katsina (1.539 mm). The mean wind speed distribution shows overall higher values in the north and lower precipitation in the south. Ikeja recorded the highest mean wind speed of 3.025 m/s at a height of 2 m, followed by Katsina (2.707 m/s) and then Maiduguri (2.605 m/s), while the lowest mean wind speed values were recorded in Asaba (0.753 m/s) and Akure (0.8297 m/s). This is as a result of the cool and moist south-westerly winds from the Atlantic Ocean which brings in more rainfall, dew, fog etc. as compared to the strong-hot, dry and dusty north-easterly winds from across the Sahara Desert into the northern part of the country separated by the Inter-Tropical Discontinuity (ITD) [31, 32].

Both the mean air temperature and all sky radiation show higher values in the north and lower values in the southern part of the country. Maiduguri has the highest mean air temperature of 28.011 °C, followed by wed by Sokoto (27.879 °C) and then Birnin Kebbi (27.615 °C). The lowest mean temperature was recorded in Jos (22.98 °C) followed by Zaria-Kaduna (24.214 °C). Jos has the lowest temperature as a result of its location which is the highest area above sea level in the country. The distribution of the all-sky solar radiation indicates that Gusau has the highest mean solar radiation value of 21.57 MJ/m^2/day Jigawa (21.18 MJ/m^2/day) in second place and Gombe (20.826 MJ/m^2/day) coming third. The lowest mean value of mean all-sky radiation was recorded in Yenagoa (10.415 MJ/m^2/day) followed by port Harcourt (10.724 MJ/m^2/day) and then Calabar (11.055 MJ/m^2/day). The moist south-western Trans-Atlantic winds create a dense cloud cover which reduces the intensity of the solar radiation in the southern part of the country as compared to the dry and hazy north-easterly winds from across the Sahara Desert which creates a clear sky in the north, exposing the region to higher solar radiation.

4.3. Spatial distribution of Correlation Dimension for the meteorological variables

The results displayed in Figure 7 show the spatial distribution of correlation dimension values of mean daily precipitation, wind speed, temperature and all sky radiation over Nigeria. The results show in general, a low dimensionality (degree of freedom) and complexity ($\nu < 5$) in the dynamics of these parameters. Surrogate testing was deployed using five surrogate data sets generated from the original time series and positive values of the S statistic were obtained in all meteorological data sampled. Hence significance levels and nonlinearity (chaotic behavior) was confirmed. The variation of correlation dimension with latitude and longitude are also displayed in Figure 8.

The Correlation Dimension trends reveal that:

1. The correlation dimension values for precipitation were observed to be in the range 0.106-2.34 which is in agreement with the values obtained by Fuwape *et al.* [7] and Echi *et al.* [6] for Makurdi. The values were observed to be lower in north and higher in the southern part of the country leading to a significantly increasing trend (Figure 8(a) and 8(b)). This is same with the actual distribution of mean precipitation across the country as the precipitation values in the northern locations has more zero values (drier weather with fewer days of rainfall) as compared to the precipitation data in the southern part which has more days of rainfall, abundant dew, fog etc. and thus lesser zero values in the data. Calabar recorded the highest correlation dimension value of 2.338, followed by Uyo (2.067) and then Port Harcourt (1.652), while the lowest values were recorded in Kano (0.106), Gusau (0.126) and Dutse (0.134). The low finite fractal value of the correlation dimension values is an indication of the presence of low dimensional deterministic chaos in the precipitation across the country [32].
2. The correlation dimension values for wind speed were computed and observed to be in the range 3.81-4.33. The values were observed to increase from west to east significantly (Figure 8(d) along increasing longitude) but with no significant trend from south to north (Figure 8(c) along increasing latitude). This may be due to the effect of the stability and abundance of

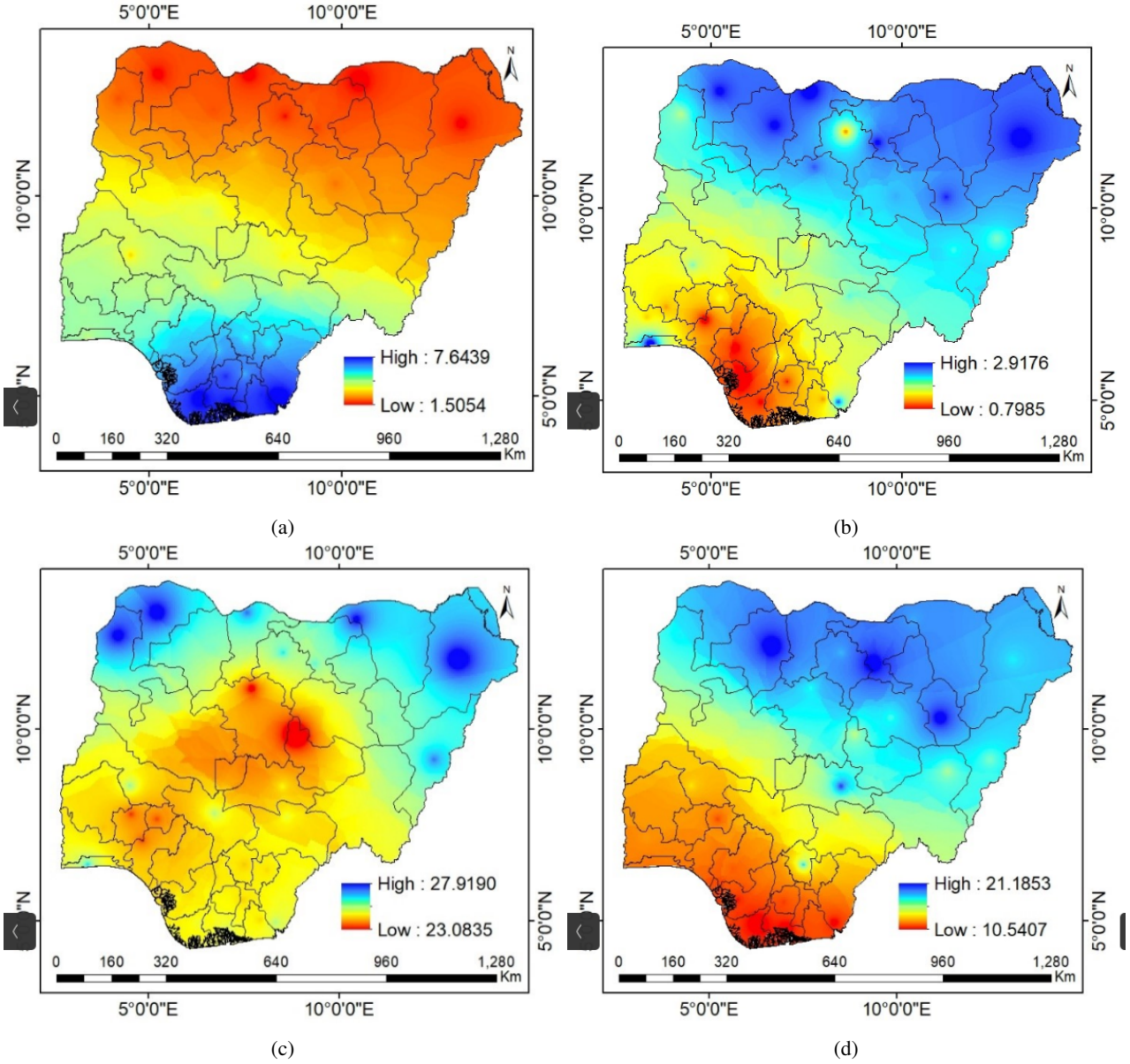

Figure 5: Spatial distribution of mean values of: (a) Precipitation (b) Wind speed (c) Temperature (d) All sky radiation across Nigeria from 1982-2020.

strong south-westerly winds from the Atlantic Ocean and north-easterly winds from across the Sahara Desert separated by the Inter-Tropical Discontinuity (ITD) whose position varies seasonally [33–35]. Port Harcourt recorded the highest correlation dimension value of 4.332, with Calabar (4.213) and Kano (4.196), while the lowest values were recorded in Ikeja (3.808), Katsina (3.827) and Ekiti (3.876), all along the western axis (longitude) of the country. The low range of correlation dimension values of wind speed implies that 4-5 degrees of freedom is required to model the wind speed dynamics across the country.

3. The correlation dimension values of air temperature displayed in Figures 8(e) & 8(f) shows insignificant trends that are not well defined, even though patches of higher values are recorded in the some southern, middle-belt and north-eastern locations. The values range from 3.55-4.26, with Ibadan having the highest value of 4.262, Yola (4.185), Gombe (4.129) and Ilorin having the lowest value of 3.554, Lafia (3.7567) and Kaduna (3.768). The effect of coastal and desert winds may also be responsible for the higher dimensions at some extreme border locations while hot spot locations which exhibit high and low correlation dimension values leading to the insignificant trends might be due to local factors such as anthropogenic effects, topography of the location etc. [7].
4. The correlation dimension values for all-sky radiation displayed in Figures 8(g) and 8(h) show insignificant trends similar to that of daily mean air temperature, with higher values recorded in the south-west and north-eastern parts of the country. The values range from 3.59-4.25, these values are slightly higher than the values obtained by Fuwape *et al.* [7] due to the effects of

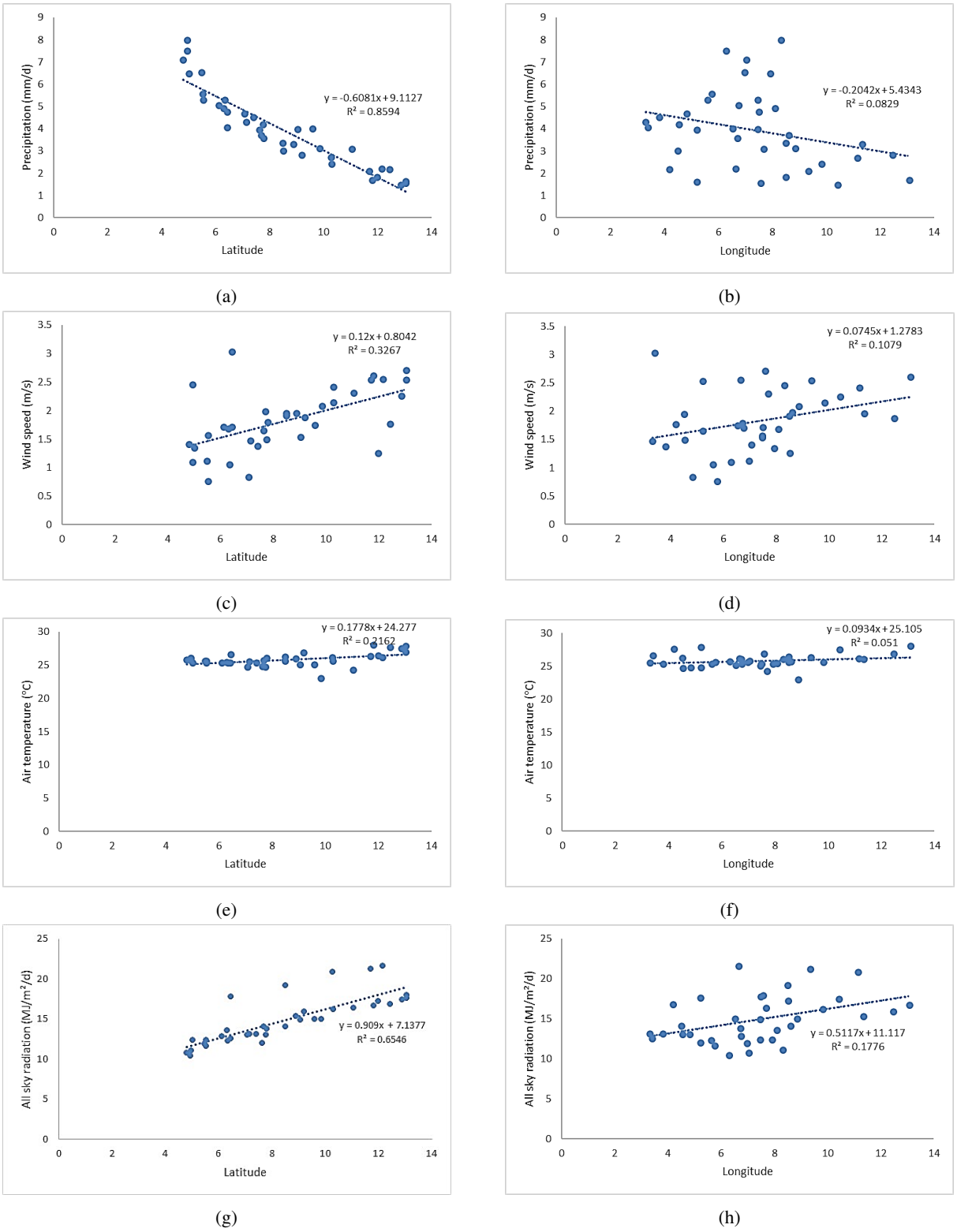

Figure 6: Variation of mean values of the meteorological variables with latitude (south to north) and longitude (west to east) over Nigeria.

climate change over the extended study period (1984-2020) and the more accurate selection of the neighborhood radius during the execution of the Grassberger-Procaccia algorithm (Figure 3). Owerri has the highest value of 4.254, Abeokuta (4.054), Ado Ekiti (4.051) While Asaba has the lowest value of 3.596, Yenagoa (3.668) and Abakiliki (3.716). Here too, the hot spots causing insignificant trends might be caused by varying scales of anthropogenic effects at these locations.

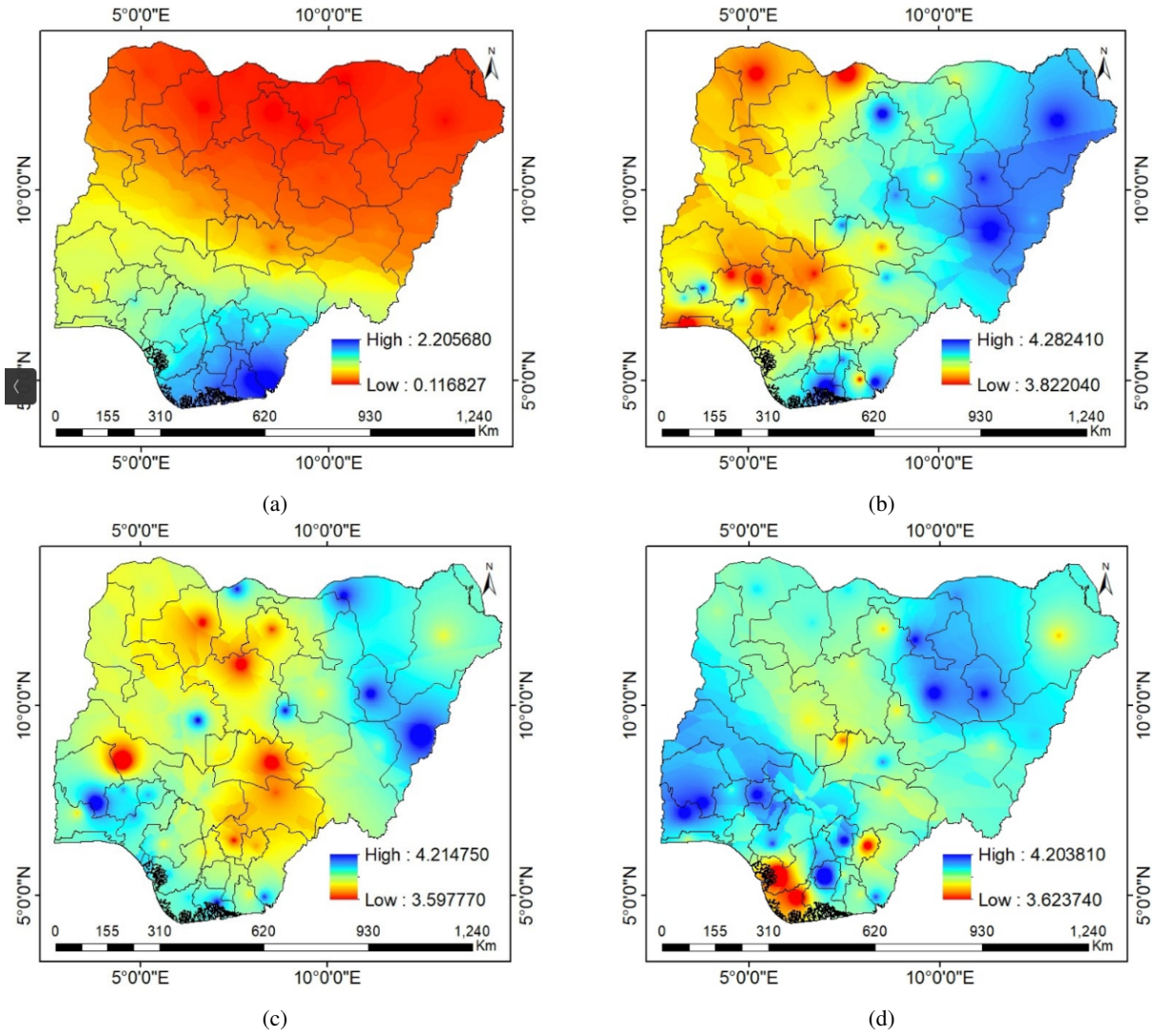

Figure 7: Spatial distribution of correlation dimension in (a) precipitation (b) wind speed (c) temperature and (d) all sky radiation over Nigeria.

4.4. Spatial distribution of the Lyapunov Exponents of the meteorological variables

The Lyapunov exponents (LE) of most of the meteorological parameters over the thirty-eight-year study period were computed and the results are displayed in spatial maps in Figure 9, with the variation with latitude and longitude illustrated in Figure 10. It is important to note that all the Lyapunov exponent values obtained are found to have positive values indicating the presence of deterministic chaos in the dynamics of the variables. This is in slight disagreement with the results obtained by Fuwape *et al.* who obtained negative Lyapunov exponents for all locations in the north for rainfall and temperature [7]. The contrast in results is as a result of the more appropriate application of Rosenstein's algorithm in this work by selecting the right expansion step from which the slope is taken to obtain the largest Lyapunov exponent and not along the whole expansion steps tentatively set while computing (Figure 4). This region selected is the expansion step after the short transition in the long rising region prior to its saturation for chaotic systems. The saturation of the curve is due to the fact that at longer times, the system is bounded in phase space and so the average exponential divergence cannot exceed the length of the attractor [22].

The Lyapunov Exponent (LE) trends reveal that:

1. The Lyapunov exponent values for precipitation in Figures 10(a) and 10(b)) show higher positive values in the north east and lower values in the south with the north west and middle belt regions exhibiting moderate values. The trend increases significantly from south to north, with values ranging from 0.00181-0.0591/day. Sokoto recorded the highest degree of chaos with an LE value of 0.0591, Jos (0.0162/day) and Bauchi (0.01574/day) while Kano on the other hand recorded the steadiest precipitation with a LE value of 0.001814/day followed by Yenagoa (0.00211/day) and Asaba (0.002639). The trend in LE of precipitation may be due to the nature of the spread in precipitation from south to north, with the southern part of Nigeria

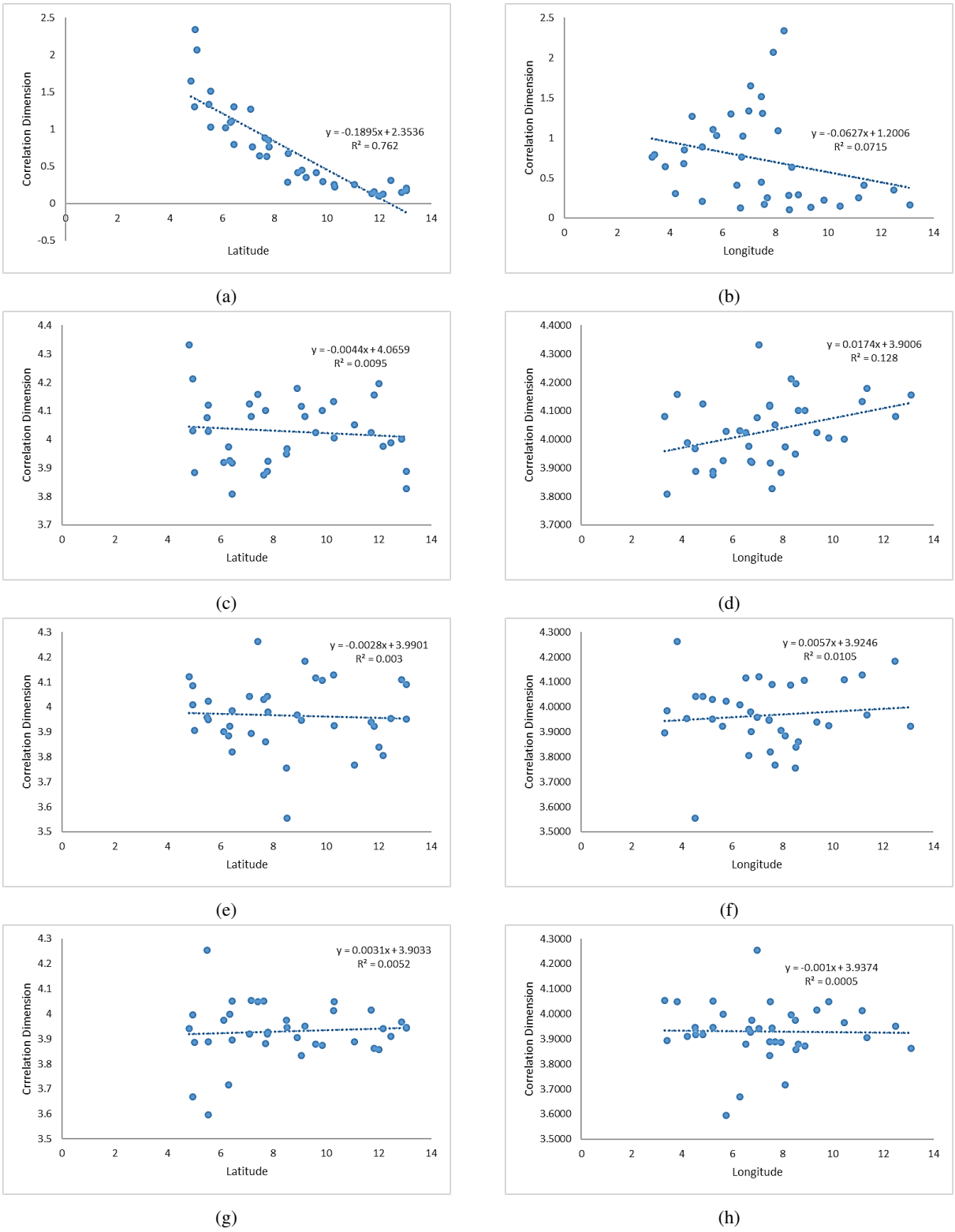

Figure 8: Variation of the correlation dimension of the meteorological variables with latitude (South to North) and longitude (West to East) across Nigeria.

experiencing more steady precipitation as a result coastal effects and the north experiencing less precipitation and higher temperatures leading to lower predictability (higher degrees of chaos), with one day of predictability lost for every 3°C rise in temperature [33, 36].

2. The Lyapunov exponent values for wind speed in Figures 10(c) and 10(d) show higher positive values in the south and lower

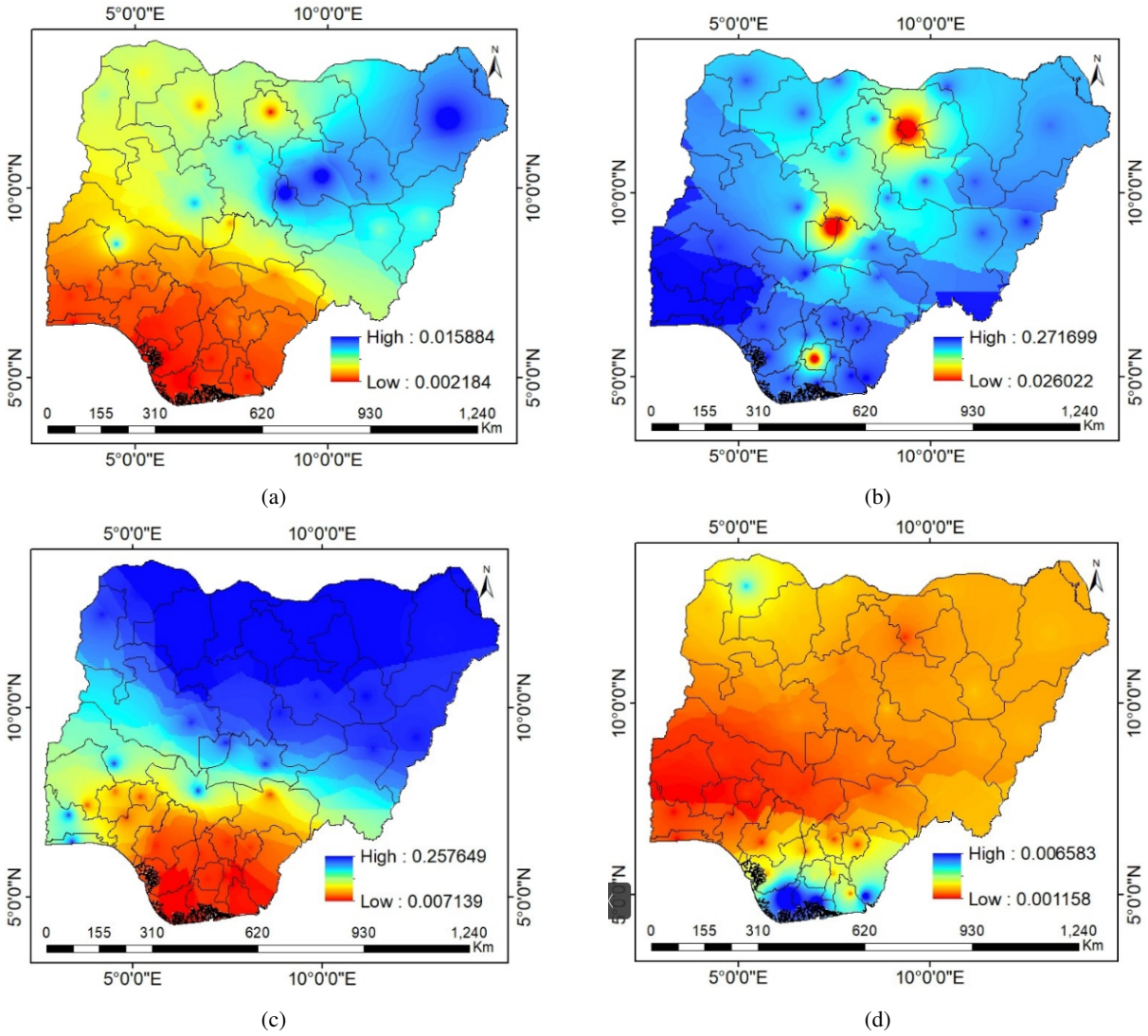

Figure 9: Spatial distribution of the Lyapunov exponents in: (a) precipitation (b) wind speed (c) temperature and (d) all sky radiation over Nigeria.

values in the north with insignificant trends from south to north (along the increasing latitude) and west to east (along increasing longitude). The LE values for wind speed are higher with values ranging from 0.00696-0.277 /day. Port Harcourt has the highest LE value of 0.2771, Calabar (0.2743 /day) and Uyo (0.274 /day) while Abuja recorded the most regular wind speed with a LE value of 0.00696 /day then Dutse (0.00898 /day) and Owerri (0.01766 /day). The high values of LE maybe due to the unstable and turbulent nature of the wind powered by varying changes in sea surface temperature (El Nino/southern oscillation) from the Atlantic Ocean in the south to the Sahara Desert in the north, as well as human anthropogenic activities leading to greenhouse effect and global warming [34, 37].

3. The spatial distribution of LE of the air temperature across Nigeria reveals a significantly higher degree of chaos in temperature as you move from the southern to northern part of Nigeria (Figure 9(c)) with patches of high values in the south-west and middle-belt region particularly in Lokoja, Ilorin, Abeokuta and Ikeja due to the fact that, higher temperature regions in midlatitude regions usually exhibit lower predictability (higher degrees of chaos), with one day of predictability lost for every 5°C rise in temperature [33, 36]. The values range from 0.00369-0.26 /day with Ikeja having the highest value of 0.260 /day, Abeokuta (0.259 /day) and Abuja (0.259 /day) while Umuahia recorded the lowest value of 0.00369, Asaba (0.00832 /day) and Ado Ekiti (0.00849 /day). The range of values is significantly lower than the values obtained by Fuwape *et al.* (0.35-1.6) [6] but within the range of values obtained by Echi *et al.* (0.00574) [6] and Millan *et al.* (0.0174) [35] with the reasons as earlier stated.
4. The spatial distribution of LE of the all-sky radiation show insignificant undefined trends across Nigeria as high values are recorded in the south-south region while the north has low values and south-west recorded the lowest values of all the regions

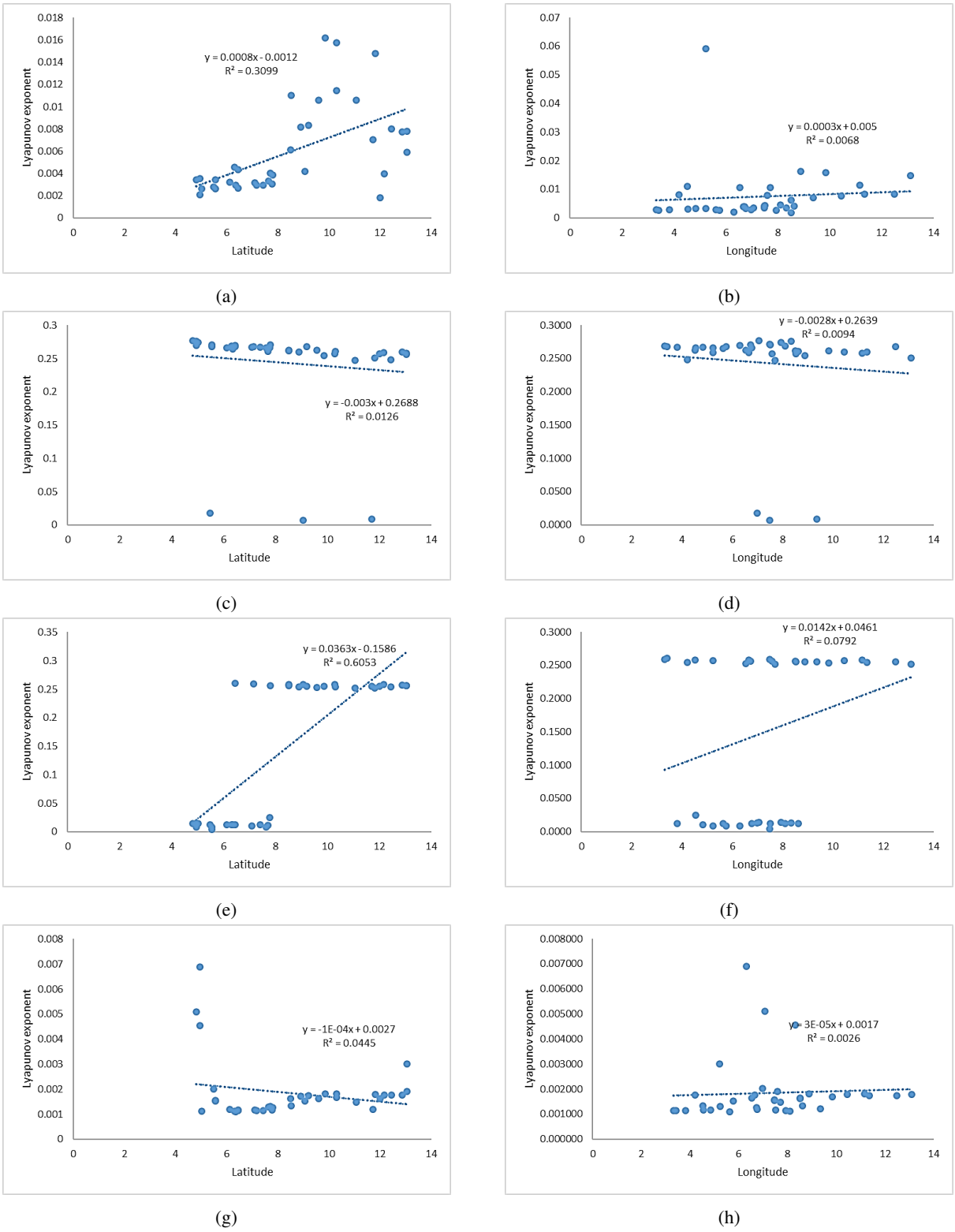

Figure 10: Variation of the Lyapunov exponents of the meteorological variables with latitude (South to North) and longitude (West to East) across Nigeria.

as shown in Figure 9(d). The values are generally low, ranging from 0.00109-0.00689 /day with Yenagoa having the highest value of 0.00689 /day Benin City recording the lowest value of 0.00109. Sokoto in the north-west also recorded a surprising higher value of 0.00301. Here too, the undefined trend may be due to local factors earlier stated, but on the whole, the all-sky radiation shows less chaotic behavior than air temperature and thus is more predictable.

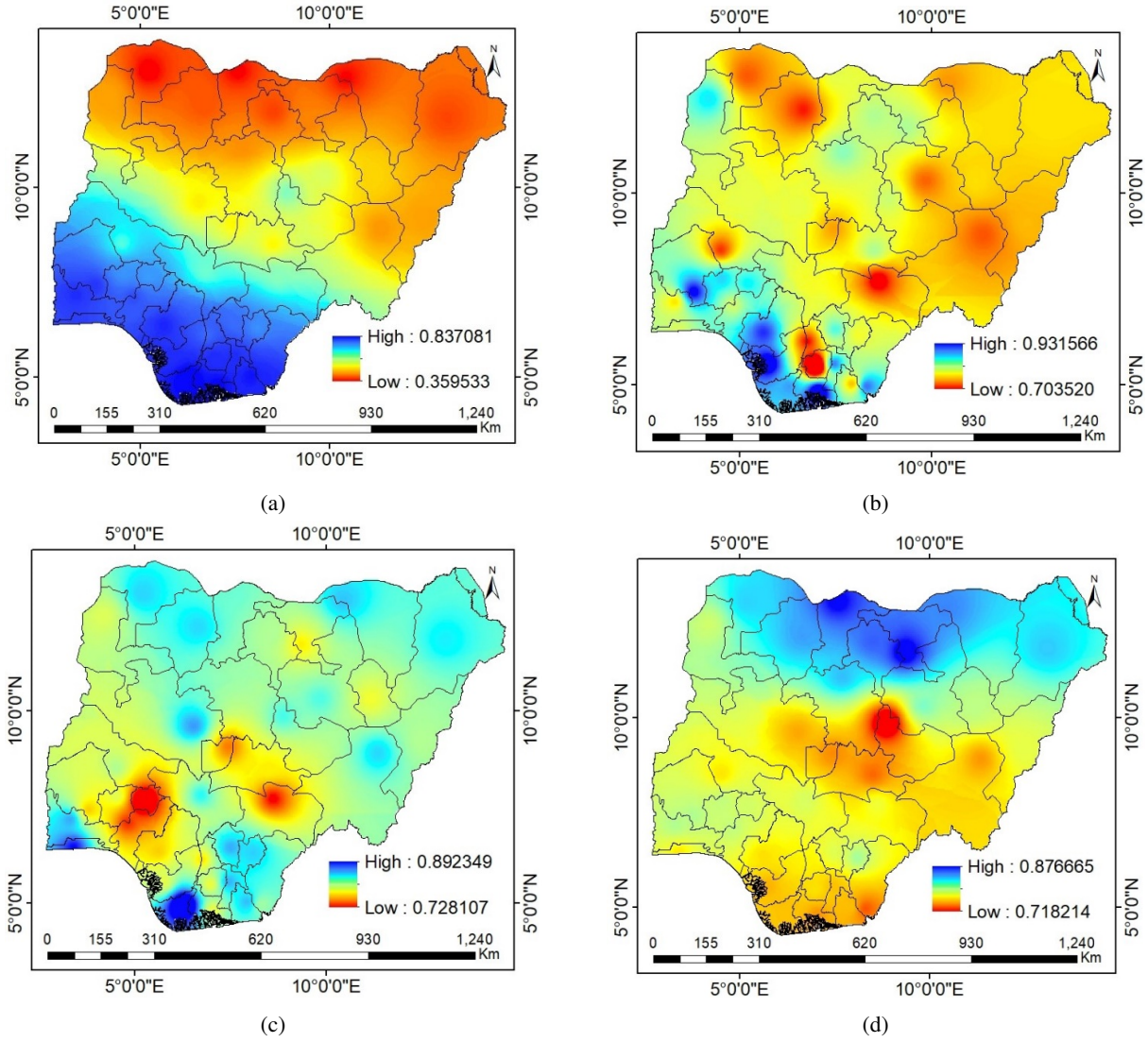

Figure 11: Spatial distribution of the Approximate entropy in: (a) precipitation (b) wind speed (c) temperature and (d) all sky radiation over Nigeria.

4.5. Spatial distribution of the Approximate Entropy of the meteorological variables

The results of the approximate entropy computation of the meteorological parameters are displayed in spatial maps in Figure 11 while the variation of approximate entropy with latitude and longitude is illustrated in Figure 12. A higher value of approximate entropy indicates a lesser degree of similar repetitive patterns in the system.

The Approximate Entropy trends reveal that:

1. The approximate entropy values for precipitation are presented in Figure 11(a) and it shows higher values in the south and lower values in the north. The value increases significantly from north to south Figure 12(a), with values ranging from 0.359-0.837. Yenagoa recorded the highest degree of irregularity in precipitation with an entropy value of 0.837, then Port Harcourt (0.824) and Uyo (0.816) while Sokoto recorded the most regular precipitation pattern with an entropy value of 0.359 followed by Katsina (0.364) and Damaturu (0.366). The trend of entropy in precipitation implies the north has been experiencing more regularly repeating pattern of precipitation over the last three decades than the southern part of the country, thus implying a higher predictability.
2. The spatial distribution of approximate entropy in wind speed displayed in Figure 11(b) shows undefined trend of values from the southern to the northern parts of the country with insignificant increasing trends from south to north (along the increasing latitude) and west to east (along increasing longitude) as shown in Figures 12(c) and 12(d). The entropy values for wind speed exhibits high values across the country implying lower degree of repetitive patterns in winds speed across the country ranging from 0.703-0.932 with Port Harcourt having the highest entropy value of 0.932, Asaba (0.915) and Ibadan (0.903)

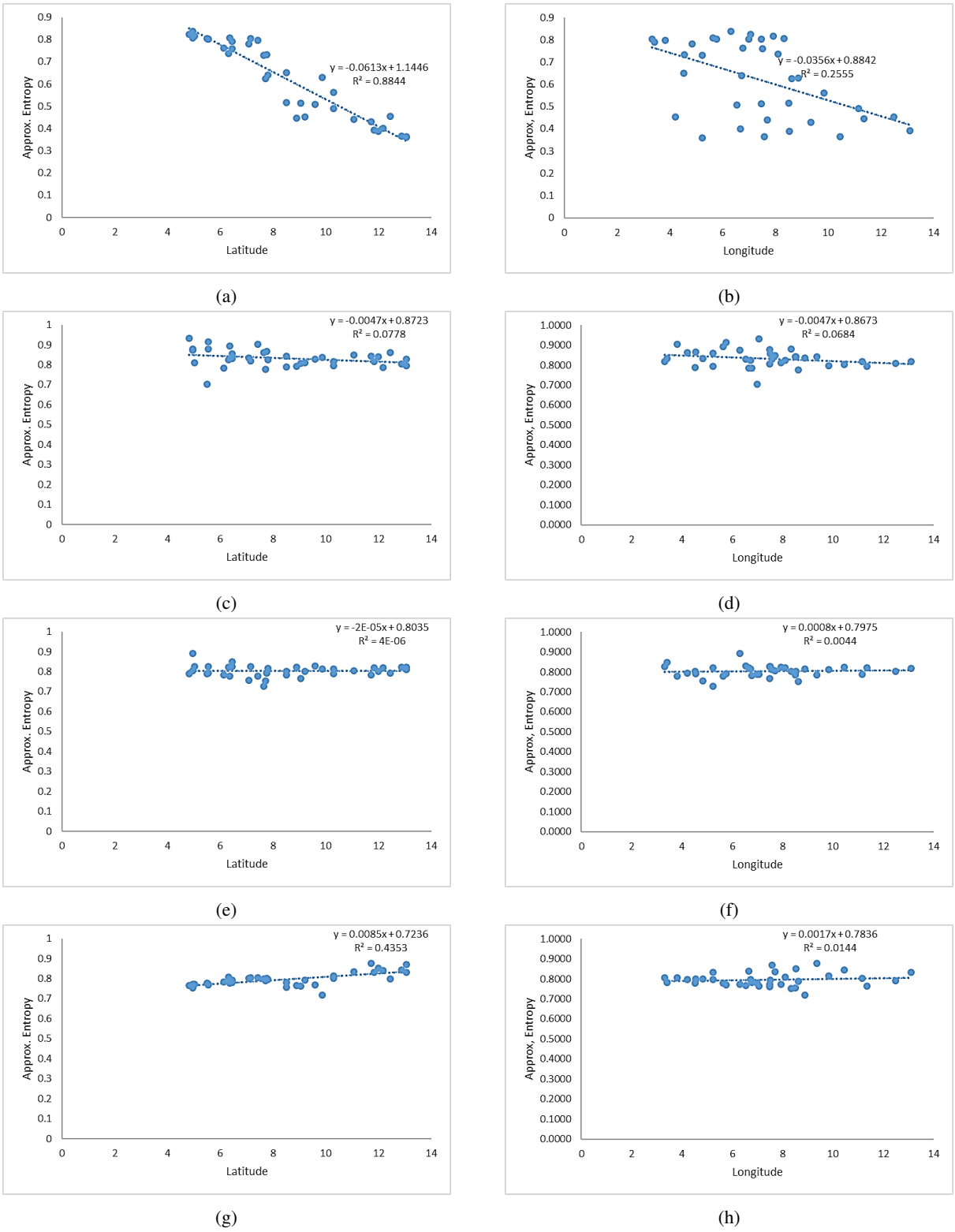

Figure 12: Variation of the Approximate entropy in the meteorological variables with latitude (South to North) and longitude (West to East) across Nigeria.

while Owerri recorded the most regular pattern of wind speed with an entropy value of 0.703, then Makurdi (0.777) and Awka (0.784). The high values of entropy maybe due to the fact air is light, has low viscosity and thus expands rapidly and randomly when in contact with hot surfaces. and since air is a poor conductor of heat, the wind easily induces forced convections leaving the weather is an unstable equilibrium at all times, hence its high approximate entropy [2]. Once again, local factors are at play

for the undefined trends.

3. The spatial distribution of approximate entropy for air temperature across Nigeria also reveals high values indicating low degree of similar repetitive patterns and undefined, insignificant trends (Figure 11(c)). Its values range from 0.724-0.892 with Yenagoa having the highest value of 0.892, Ikeja (0.848) and Minna (0.829) while Ado Ekiti has the lowest value of 0.728 followed by Makurdi (0.753) and then Akure (0.756).
4. The spatial distribution of approximate entropy in all-sky radiation in Figure 11(d) shows higher values in the north and lower values in the south with significant increasing trends (Figures 12(g) and 12(h)) across Nigeria. Here too the values generally show high degree of non-repetitive patterns, ranging from 0.718-0.877 with Dutse having the highest value of 0.877, then Katsina (0.868) and Kano (0.851) while Jos recorded the lowest value of 0.718 due to its high altitude location, followed by Calabar (0.753) and then Lafia (0.756). Climate change (global warming) as a result of local anthropogenic activities such as greenhouse gas emission from industries, refineries, exhaust gases from vehicles and use of pesticides and herbicides during agricultural activities etc. may be responsible for the high degree of irregular non-repetitive patterns in air temperature and all-sky radiation across the country over the last three decades [33, 36].

5. Conclusions

This research applied the tools of nonlinear dynamical analysis to meteorological data collected over the thirty-seven locations across Nigeria in order to characterize the data and also determine the degree and spatial distribution of chaos in Nigeria's weather over the last three decades using some quantitative tools of nonlinear analysis which include: correlation dimension, Lyapunov exponents and approximate entropy. Results obtained from the analysis confirms the presence of low dimensional deterministic chaos in the climate across Nigeria from 1982-2020 as all the Lyapunov exponents were positive, with the northern part requiring lower degrees of freedom (correlation dimension value) to model the precipitation and air temperature, but higher degrees of freedom to model the wind speed and all sky radiation in the region. The southern part of Nigeria on the other hand requires higher degrees of freedom to model the precipitation, temperature and all-sky radiation but requires lower degrees of freedom to model the wind speed in region. It was also observed that the north has higher degree of chaos in precipitation and air temperature as reflected in the higher values of the Lyapunov exponents (increase latitudinally) while the southern part of the country exhibits more chaotic dynamics in wind speed and all-sky radiation (decreases with latitude). This is due to the fact that warmer weather tends to be less predictable and so as climate change and global warming sets in, the temperature and precipitation in the north tends to become more chaotic and less predictable [33, 36]. Furthermore, precipitation and wind speed exhibits more steady repetitive pattern in the north over the years while air temperature and all-sky radiation show less repetitive patterns along border locations in the far north and coastal locations in the south-south region. These chaotic trends are attributed to local effects such as human anthropogenic activities (greenhouse gas emissions), topography of these locations and variations in the position of the Inter-Tropical Discontinuity as a result of the El Nino/Southern Oscillations (ENSO), as the equatorial ocean-atmosphere oscillator usually goes into nonlinear resonance with the seasonal cycle and the strong coupling between the ocean and the atmosphere leads to chaotic behavior as a result of irregular jumping of the ocean-atmosphere system among different nonlinear resonances [34, 37]. It is recommended that smart alternative technologies by way of advanced irrigation be developed and applied for agricultural processes across the country. This will go a long way in ensuring the regular supply of water for a more reliable crop yield and all year round crop production. Renewable energy resources should be harnessed more for power generation. These will ensure that the government's efforts towards adequate food security, regulation of greenhouse gas emissions from the burning of fossil fuels for power generation and diversification of the economy does not end in futility as a result of chaotic weather and climate change.

Data availability

Data will be made available upon reasonable request from the corresponding author.

Acknowledgment

The authors wish to acknowledge the authorities of Joseph Sarwuan Tarka University, Makurdi (JOSTUM) for their support and the Modern Era Retrospective Reanalysis (MERRA-2) for granting us access to their meteorological database in the course of this work.

References

[1] E. N. Lorenz, "Deterministic nonperiodic flow", in *The theory of chaotic attractors*, B. R. Hunt, T. Y. Li, J. A. Kennedy & H. E. Nusse (Eds.), Springer, New York, NY, USA, 2004, pp. 1. https://doi.org/10.1007/978-0-387-21830-4_2.

[2] X. Zeng, "Chaos theory and its application in the atmosphere", Dept. of Atmos. Sci., Colorado State University, Fort Collins, Paper No. **504** (1992) 5. https://mountainscholar.org/bitstream/handle/10217/32305/0504_Bluebook.pdf.

[3] A. Sharma & U. Datta, "A weather forecasting system using concept of soft computing: a new approach", AIP Conf. Proc. **923** (2007) 275. https://doi.org/10.1063/1.2767047.

[4] G. H. R. Joice & K. Thamilhazan, "Impact of tsunami on Tamil Nadu monsoon rainfall", APRN J. Sci. Technol. **2** (2012) 96. https://citeseerx.ist.psu.edu/document?repid=rep1&type=pdf&doi=a607e33f2cff92bb37dcbeddf9eaac2ec5d27135#:~:text=The%20Lyapunov%20exponent%20value%20for,are%20showing%20a%20chaotic%20behaviour.

[5] T. Fathima & V. Jothiprakash, "Behavioural analysis of a time series-a chaotic approach", Project Saadhana **39** (2014) 659. https://doi.org/10.1007/s12046-014-0249-2.

[6] I. M. Echi, E. V. Tikyaa & B. C. Isikwue, "Dynamics of rainfall and temperature in Makurdi", Int. J. Sci. Res. **4** (2015) 493. https://doi.org/10.21275/SUB156176.

[7] I. A. Fuwape, S. T. Ogunjo, S. S. Oluyamo & A. B. Rabiu, "Spatial variation of deterministic chaos in mean daily temperature and rainfall over Nigeria", Theor. Appl. Climatol. **130** (2016) 119. https://doi.org/10.1007/s00704-016-1867-x.

[8] S. Ogunjo, I. Fuwape, S. Oluyamo & B. Rabiu, "Spatial dynamical complexity of precipitation and temperature extremes over Africa and South America", Asia-Pac. J. Atmos. Sci. **60** (2019) 15. https://doi.org/10.1007/s13143-019-00131-y.

[9] A. T. Adewole, E. O. Falayi, T. O. Roy-Layinde & A. D. Adelaja, "Chaotic time series analysis of meteorological parameters in some selected stations in Nigeria", Sci. Afr. **10** (2020) e00617. https://doi.org/10.1016/j.sciaf.2020.e00617.

[10] S. Ogunjo, A. Olusola, I. Fuwape & O. Durowoju, "Temporal variation in deterministic chaos: the influence of Kainji dam on downstream stations along lower Niger River", Arab. J. Geosci. **15** (2022) 237. https://doi.org/10.1007/s12517-021-09297-0.

[11] F. Takens, "Detecting strange attractors in turbulence", Lect. Notes Math. **898** (1981) 366. https://doi.org/10.1007/BFb0091924.

[12] N. Packard, J. Crutchfield, J. Farmer & R. Shaw, "Geometry from a time series", Phys. Rev. Lett. **45** (1980) 712. https://doi.org/10.1103/PhysRevLett.45.712.

[13] A. M. Fraser & H. L. Swinney, "Independent coordinates for strange attractors from mutual information", Phys. Rev. A **33** (1986) 1134. https://doi.org/10.1103/PhysRevA.33.1134.

[14] M. B. Kennel, R. Brown & H. D. Abarbanel, "Determining embedding dimension for phase-space reconstruction using a geometrical construction", Phys. Rev. A **45** (1992) 3403. https://doi.org/10.1103/PhysRevA.45.3403.

[15] J. Theiler, "Efficient algorithm for estimating the correlation dimension from a set of discrete points", Phys. Rev. A **36** (1987) 44. https://doi.org/10.1103/PhysRevA.36.4456.

[16] W. Caesarendra, P. Kosasih, K. Tieu & C. Moodie, "An application of nonlinear feature extraction-a case study for low speed slewing bearing condition monitoring and prognosis", IEEE/ASME Int. Conf. Adv. Intell. Mechatron., Wollongong, NSW, Australia **2013** (2013) 1713. https://doi.org/10.1109/AIM.2013.6584344.

[17] D. Kaplan & L. Glass, *Understanding nonlinear dynamics*, Springer, New York, USA, 1995, pp. 278. https://doi.org/10.1007/978-1-4612-0823-5.

[18] M. Y. Boon, B. I. Henry, C. M. Suttle & S. J. Dain, "The correlation dimension: a useful objective measure of the transient visual evoked potential?", J. Vis. **8** (2008) 6. https://doi.org/10.1167/8.1.6.

[19] P. Grassberger & I. Procaccia, "Characterization of strange attractors", Phys. Rev. Lett. **50** (1983) 346. https://doi.org/10.1103/PhysRevLett.50.346.

[20] F. Mitschke & M. Dammig, "Chaos versus noise in experimental data", Int. J. Bifurcat. Chaos **3** (1993) 693. https://doi.org/10.1142/S021812749300060X.

[21] D. Prichard & J. Theiler, "Generating surrogate data for time series with several simultaneously measured variables", Phys. Rev. Lett. **73** (1994) 951. https://doi.org/10.1103/PhysRevLett.73.951.

[22] M. Rosenstein, J. J. Collins & C. De Luca, "A practical method for calculating largest Lyapunov exponents from small data sets", Phys. D **65** (1993) 117. http://doi.org/10.1016/0167-2789(93)90009-P.

[23] S. M. Pincus, "Approximate entropy as a measure of system complexity", Proc. Natl. Acad. Sci. USA **88** (1991) 2297. https://doi.org/10.1073/pnas.88.6.2297.

[24] U. R. Acharya, F. Molinari, S. V. Sree, S. Chattopadhyay, N. Kwan-Hoong & J. S. Suri, "Automated diagnosis of epileptic EEG using entropies", Biomed. Signal Process. Control **7** (2012) 401. https://doi.org/10.1016/j.bspc.2011.07.007.

[25] Worldmeters, "World population prospects: the 2015 revision", (2017). [Online]. Retrieved from http://www.worldmeters.info.

[26] M. P. Lewis, F. S. Gary & D. F. Charles, *Ethnologue: languages of the world*, SIL International, Dallas, Texas, USA, 2017. http://www.ethnologue.com/country/ng.

[27] D. S. Ragatoa, K. O. Ogunjobi, N. A. B. Klutse, A. A. Okhimamhe & J. O. Eichie, "A change comparison of heat wave aspects in climatic zones of Nigeria", Environ. Earth Sci. **78** (2019) 111. https://doi.org/10.1007/s12665-019-8112-8.

[28] R. Gelaro, W. McCarty, M. J. Suárez, R. Todling, A. Molod, L. Takacs, C. Randles, A. Darmenov, M. G. Bosilovich, R. Reichle, K. Wargan, L. Coy, R. Cullather, C. Draper, S. Akella, V. Buchard, A. Conaty, A. da Silva, W. Gu, G. K. Kim, R. Koster, R. Lucchesi, D. Merkova, J. E. Nielsen, G. Partyka, S. Pawson, W. Putman, M. Rienecker, S. D. Schubert, M. Sienkiewicz & B. Zhao, "The modern-era retrospective analysis for research and applications, version 2 (MERRA-2)", J. Clim. **30** (2017) 5419. https://doi.org/10.1175/JCLI-D-16-0758.1.

[29] D. Kwiatkowski, P. C. B. Phillips, P. Schmidt & Y. Shin, "Testing the null hypothesis of stationarity against the alternative of a unit root: how sure are we that economic time series have a unit root?", J. Econom. **54** (1992) 159. https://doi.org/10.1016/034-4076(92)90104-Y.

[30] P. Jain & M. D. Flannigan, "Comparison of methods for spatial interpolation of fire weather in Alberta, Canada", Can. J. For. Res. **47** (2017) 1646. https://doi.org/10.1139/cjfr-2017-0101.

[31] African Center of Meteorological Applications for Development (ACMAD), "Climatic and environmental conditions over Africa", Clim. Health Bull. **5** (2012). [Online]. Retrieved from http://acmad.org.

[32] P. C. Oguntunde, B. Abiodun & G. Lischeid, "Spatial and temporal temperature trends in Nigeria, 1901-2000", Meteorol. Atmos. Phys. **118** (2012) 95. https://doi.org/10.1007/s00703-012-0199-3.

[33] A. Sheshadri, M. Borrus, M. Yoder & T. Robinson, "Midlatitude error growth in atmospheric GCMs: the role of eddy growth rate", Geophys. Res. Lett. **48** (2021) 1. https://doi.org/10.1029/2021/GL096126.

[34] E. Tiperman, L. Stone, M. A. Cane & H. Jarosh, "El Nino chaos: overlapping of resonances between the seasonal cycle and the Pacific Ocean-atmosphere oscillator", Science **264** (1994) 72. https://doi.org/10.1126/science.264.5155.72.

[35] H. Millan, B. Ghanbarian-Alavijeh & I. Garcia-Fornaris, "Non-linear dynamics of mean daily temperature and dewpoint time series at Balolsar, Iran, 1961-2005", Atmos. Res. **98** (2010) 89. https://doi.org/10.1016/j.atmosres.2010.06.001.

[36] J. Garthwaithe, "Climate of chaos: why warming makes weather less predictable", Stanford Earth Matters: Clim. Change Nat. Matters. [Online]. Retrieved from https://earth.stanford.edu/news/climate-chaos-why-warming-makes-weather-less-predictable on 23/6/2022.

[37] F. Jin, J. D. Neelin & M. Ghil, "El Nino on the devil's staircase: annual subharmonic steps to chaos", Science **264** (1994) 70. https://doi.org/10.1126/science.264.5155.70.